ORNL/CP-94704

CONF-9710100--

TRANSPORT PHYSICS IN REVERSED SHEAR PLASMAS

F.M. LEVINTON[1], S.H. BATHA[1], M.A. BEER[2], M.G. BELL[2], R.E. BELL[2], R.V. BUDNY[2], C.E. BUSH[3], P.C. EFTHIMION[2], E. MAZZUCATO[2], R. NAZIKIAN[2], H.K. PARK[2], A.T. RAMSEY[2], G.L. SCHMIDT[2], S.D. SCOTT[2], E.J. SYNAKOWSKI[2], G. TAYLOR[2], S. VON GOELER[2], M.C. ZARNSTORFF[2]

[1]Fusion Physics and Technology, Inc., Torrance, California

[2]Plasma Physics Laboratory, Princeton University, Princeton, New Jersey

[3]Oak Ridge National Laboratory, Oak Ridge, Tennessee

United States of America

Abstract

TRANSPORT PHYSICS IN REVERSED SHEAR PLASMAS.

Reversed magnetic shear is considered a good candidate for improving the tokamak concept because it has the potential to stabilize MHD instabilities and reduce particle and energy transport. With reduced transport, the high pressure gradient would generate a strong off-axis bootstrap current and could sustain a hollow current density profile. Such a combination of favorable conditions could lead to an attractive steady-state tokamak configuration. Indeed, a new tokamak confinement regime with reversed magnetic shear has been observed on the Tokamak Fusion Test Reactor (TFTR) where the particle, momentum, and ion thermal diffusivities drop precipitously, by over an order of magnitude. The particle diffusivity drops to the neoclassical level and the ion thermal diffusivity drops to much less than the neoclassical value in the region with reversed shear. This enhanced reversed shear (ERS) confinement mode is characterized by an abrupt transition with a large rate of rise of the density in the reversed shear region during neutral beam injection, resulting in nearly a factor of three increase in the central density to $\sim 1.2 \times 10^{20}$ m^{-3}. At the same time the density fluctuation level in the reversed shear region dramatically decreases. The ion and electron temperatures, which are about 20 keV and 7 keV respectively, change little during the ERS mode. The transport and transition into and out of the ERS mode have been studied on TFTR with plasma currents in the range 0.9–2.2 MA, with a toroidal magnetic field of 2.7–4.6 T, and the radius of the $q(r)$ minimum, q_{min}, has been varied from r/a = 0.35 to 0.55. Toroidal field and co/counter neutral beam injection toroidal rotation variations have been used to elucidate the underlying physics of the transition mechanism and power threshold of the ERS mode.

DISCLAIMER

1. Introduction

The economic attractiveness of the tokamak as a candidate for a fusion reactor depends on development of a magnetic configuration that has good confinement, stability, and low recirculating power for steady state current drive. This requires a high fraction of self-sustaining bootstrap current that is well aligned with an optimized current density profile for confinement and stability. Recent studies[1] of the optimization of the current density profile suggest that reversed magnetic shear (i.e., a hollow current density profile), is desirable for confinement, stability, and bootstrap alignment. Shear is defined as $s \equiv (2V/q)(dq/d\psi)(d\psi/dV) \approx (r/q)(dq/dr)$, where ψ is the enclosed poloidal flux, V is the enclosed volume, q is the safety factor and r is the minor radius. Reversed shear, $s < 0$, is thought to be important because it can stabilize some classes of microinstabilities such as trapped electron modes[2,3], a candidate which may explain the observed anomalous electron transport in tokamaks. Reversed magnetic shear can also stabilize some magnetohydrodynamic (MHD) instabilities such as ballooning modes[4] and resistive tearing modes. If improved core confinement can be attained, the high pressure gradient would generate a strong off-axis bootstrap current which may sustain the hollow current density profile. This scenario may lead to an attractive concept for a steady state tokamak reactor[5]. Most tokamaks operate with inductive current drive which normally produces a peaked current density profile at the magnetic axis due to the strong dependence of the plasma conductivity on the electron temperature. Only by non-inductive current drive or transient techniques can a hollow current density profile be generated. This has been done in several experiments reporting improved confinement[6–8] and stability[9]. In addition, several other experiments have reported the stabilization of MHD modes in the high β_p regime[10–12].

Recent experiments on the Tokamak Fusion Test Reactor (TFTR)[13] have demonstrated a reversed shear configuration with greatly improved particle and ion thermal transport[5,14] in the reversed shear region that is more than an order of magnitude lower than reported in previous experiments, including reversed shear experiments. The $q(R,t)$ profile is obtained from the motional Stark effect (MSE) polarimeter[15,16] measurement of the local magnetic field pitch, in contrast to the indirect methods used in many previous experiments. The diagnostic provides good temporal and spatial resolution and shows the correlation of the magnetic shear with changes in transport. This regime of operation holds promise for significantly improving the tokamak reactor concept and can lead to a dramatic increase in the performance of present tokamaks.

2. Reversed Shear Formation

With the use of early neutral beam injection (NBI) to heat the plasma and drive current a reversed shear $q-$profile can be obtained. The early NBI heat-

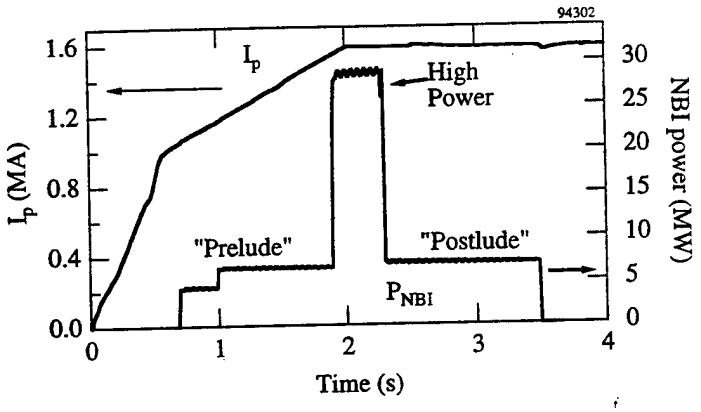

FIG. 1. Plasma current and neutral beam power for a 1.6 MA reversed shear discharge.

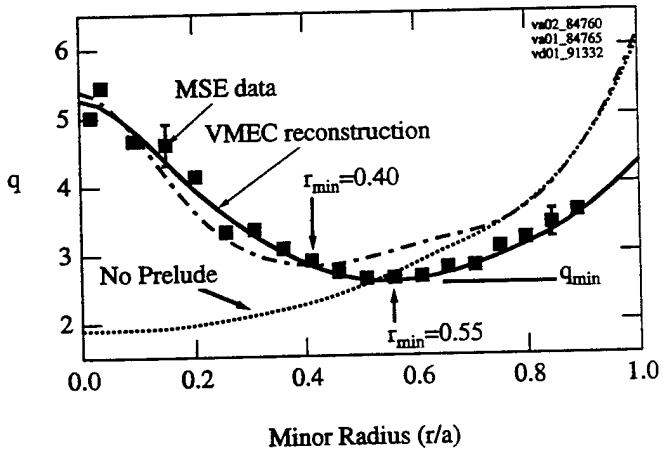

FIG. 2. q-profiles at the beginning of the current flattop at $t = 2$ s for a 1.6 MA startup (dashed–dotted line), a fast ramp 2.2 MA startup (solid line) with MSE data and a case with no early NBI heating phase (dotted line).

ing during the plasma current ramp phase increases the electron temperature to several kilo-electronvolts and the current penetration time increases to ~ 10 seconds, resulting in a hollow current density profile and a reversed shear $q-$profile that can be maintained for several seconds. The plasma current is initially increased at a ramp rate of 1.8 MA/s to about 1.0 MA and then at a reduced rate until the final plasma current is reached, as shown in Fig. 1. With variations of the rate of rise of the plasma current and timing of the neutral beam injection a wide range of $q-$profile minima, q_{min}, and q_{min} radii, r_{min}, can be generated

for transport and stability studies. In the plasmas discussed here the major radius is 2.60 m, the minor radius is 0.94 m, and the toroidal field is 4.6 T with an edge safety factor of $\sim 6.2 - 4.3$ corresponding to plasma currents of 1.6-2.2 MA. Plasmas at lower toroidal field with $q(a) \sim 6.2$ have also been investigated. Typical q-profiles resulting from different current ramp rates and NBI timing are shown in Fig. 2. The profiles have been reconstructed with the VMEC free-boundary equilibrium code[17] from MSE data, kinetic pressure data, calculated fast ion pressure from the TRANSP code[18], and external magnetic data. The uncertainties in $q(R)$ are 10% or less across the profile[19]. The MSE analysis for these $q(R)$ profiles includes corrections due to the plasma radial electric field E_r [20]. The quantities $q(0)$, q_{min}, and r_{min} slowly decrease on a time scale of several seconds and reach $q(0) \sim 3 - 4$, $q_{min} \sim 2$, and $r_{min}/a \sim 0.3 - 0.5$ after three seconds of beam heating, consistent with the neoclassical current diffusion rate and the calculated driven currents.

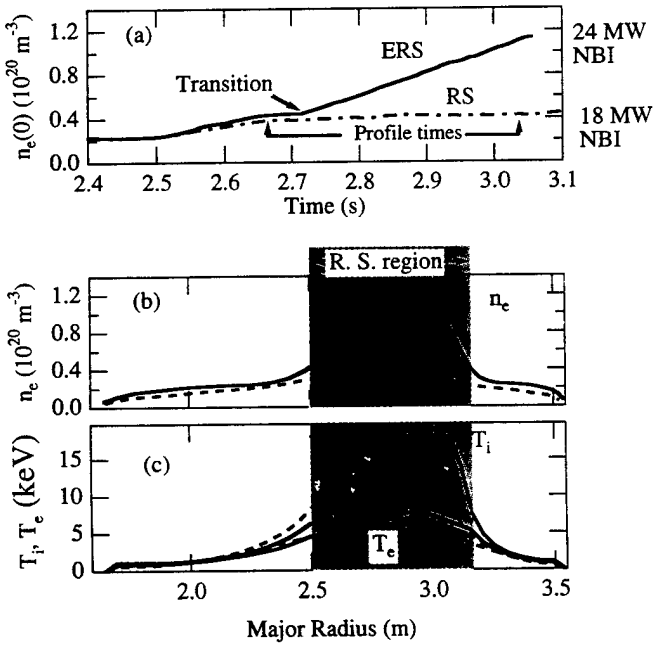

FIG. 3. (a) Evolution of the central density for a discharge that makes a transition into the ERS-mode at 2.715 s (solid line) and a similar reversed shear discharge at lower NBI power which does not (dashed-dotted line). (b) Density and (c) temperature profiles before a transition into the ERS-mode (dashed line) and at the time of peak density (solid line).

3. ERS-Mode Characterization

Below NBI powers of 18 MW, the plasmas formed in the reversed shear configuration appear to be similar to supershots[21], with a central ion temperature of $\sim$ 24 keV, electron temperature of $\sim 6-8$ keV and a central electron density of $\sim 4\times10^{19}$ m^{-3}. However, above an empirical threshold in neutral beam power, in the range of $\sim$ 18-30 MW, the particle and thermal transport dramatically improve in the plasma core where the shear is reversed. The transition to the highly peaked, enhanced reversed shear (ERS) mode occurs abruptly during the discharge, within 0.1-0.9 seconds after the start of the high power heating phase. Shown in Fig. 3(a) is the evolution of the central density, with a transition into the ERS-mode at $t = 2.715$ s. Also shown in Fig. 3(a) is a discharge without an ERS-mode transition, which has slightly lower NBI power and similar reversed shear q-profile. The electron density profile is shown in Fig. 3(b) at two times, just before the transition into the ERS-mode and near the time of peak density. The corresponding electron and ion temperature profiles are shown in Fig. 3(c).

When the radius of q_{min} is increased, the density and temperature profiles are broadened. In Fig. 4(a) is the $q-$profile for a typical ERS discharge at the time of peak beta compared to an ERS discharge formed with a faster plasma

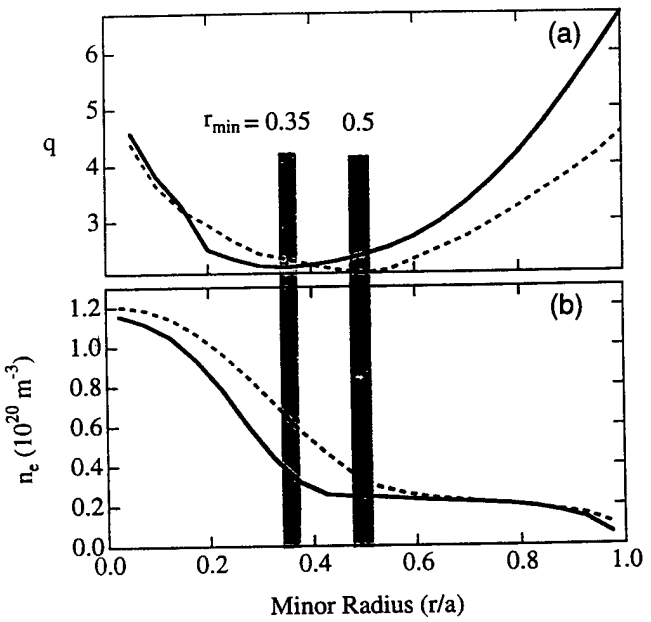

FIG. 4. (a) q-profiles with r_{min} at r/a = 0.35 (solid line) and r/a = 0.5 (dashed line) along with the corresponding (b) density profiles.

current ramp-up which results in a larger r_{min}. The corresponding electron density profiles are shown in Fig. 4(b). Similarly the temperature profiles are broader and the particle and ion thermal diffusivity profiles have a wider region of reduced transport, demonstrating the correlation of reversed shear with the reduction of particle and thermal transport.

4. Particle Transport

The effects on local transport by the ERS-mode are assessed with the $1\frac{1}{2}$-D time-dependent code, TRANSP, using experimentally measured temperature, density, and $q-$profiles. The $T_e(R,t)$ profile is measured by electron cyclotron emission (ECE), $T_i(R,t)$ and toroidal rotation by charge-exchange emission spectroscopy, $n_e(R,t)$ by a ten-channel far-infrared interferometer array, $q(R,t)$ is measured by MSE, and Z_{eff} is calculated using a tangential visible bremsstrahlung array. After the transition into the ERS-mode, the inferred particle and ion thermal diffusivity drop precipitously throughout the region of reversed shear, which extends out to $r/a \sim 0.35$. The improved confinement extends beyond the reversed shear radius, into the region of reduced shear as well. The inferred particle diffusivity, D_e, assuming no pinch terms, drops by a factor of ~ 40 in the reversed shear region to roughly the neoclassical level or perhaps lower, as shown in Fig. 5. The low value of the electron particle diffusivity has been found to persist for several hundred milliseconds after the neutral beam power is reduced substantially to 5 MW in a low power "postlude" phase. This reduces the uncertainty of the inferred particle diffusivity, since the the terms that determine the flux in the particle balance equation, the neutral beam source of particles and density rate of rise, are much smaller, and hence the uncertainty arising from their difference is much lower.

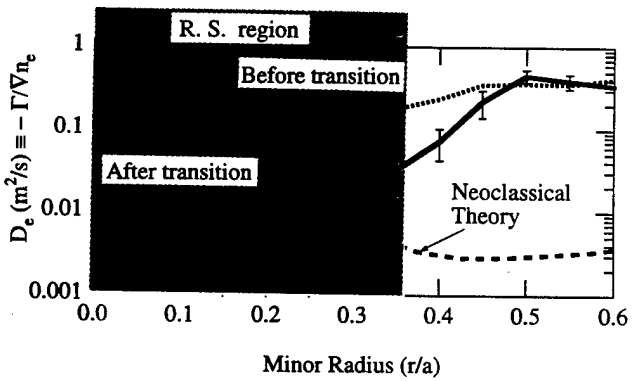

FIG. 5. Electron particle diffusivity profile before a transition (dotted line) at 2.6 s and after a transition (solid line) at 3.0 s with the estimated neoclassical particle diffusivity (dashed line). The reversed shear region extends to r/a ~ 0.35.

Along with the reduction of particle transport, a reduced level of density fluctuations is measured by a microwave reflectometer. Both the temporal evolution and spatial location of the reduced fluctuation level coincide with the reduction in particle transport[22].

TFTR is uniquely equipped to study hydrogenic ion transport using non-perturbing tritium puffs at the plasma edge, and observing the D-T neutrons with a 12 channel neutron collimator. The tritium density is inferred from the neutrons. A perturbation analysis is used to determine the diffusivity and convective velocity profiles. Due to the much larger cross section for D-T compared to D-D fusion and higher detector sensitivity to D-T neutrons, the tritium puff can be quite small and perturbs the density by about 1%. This technique had previously been developed on TFTR for studying hydrogenic transport in supershots[23]. A similar analysis in the ERS-mode finds the tritium diffusivity in the reversed shear region to be much lower than outside r_{min} and is comparable to that predicted by neoclassical theory. The helium profile evolution, measured with charge exchange recombination spectroscopy, from a small gas puff is similar to the tritium puff results and also indicates that the diffusive transport is markedly reduced inside r_{min} as compared to outside.

5. Thermal Transport

In ERS plasmas the ion power balance has little convective loss since the particle diffusivity is so small. This is in contrast to typical supershot discharges on TFTR which are dominated by convective loss in the plasma core[24]. However,

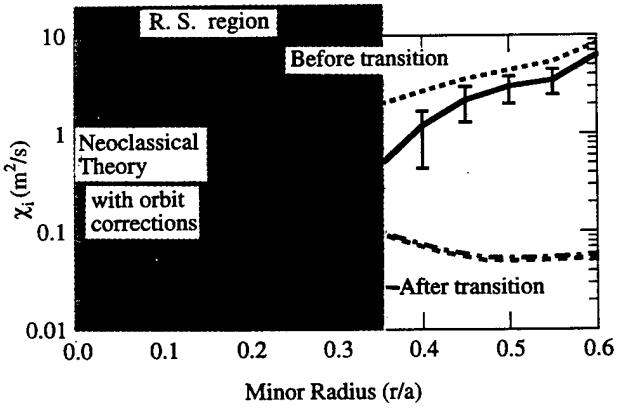

FIG. 6. Ion thermal diffusivity profile before a transition (dotted line) at 2.6 s and after a transition (solid line) at 3.0 s, and the neoclassical ion thermal diffusivity (dashed line) including orbit corrections (dashed-dotted line). The reversed shear region extends to r/a ~ 0.35.

in ERS plasmas the ion power balance does have a large loss from electron-ion energy exchange, $q_{ie} = 3n_i\nu_e\frac{m_e}{m_i}(T_i - T_e)$, where n_i is the ion density, ν_e is the electron collision frequency, $m_{e(i)}$ is the electron (ion) mass and $T_{e(i)}$ is the electron (ion) temperature. This is due to the large difference between the ion and electron temperatures and the large central density. Assuming classical electron-ion energy exchange and no pinch term it is found that the ion thermal diffusivity, χ_i, drops substantially to a level that is much less than the estimated neoclassical[25] value, χ_i^{nc}, which is widely believed to be the irreducible minimum transport possible. Profiles of the inferred ion thermal diffusivity, before and after a transition into the ERS-mode compared to estimated neoclassical ion thermal diffusivity, are shown in Fig. 6. It is quite remarkable that the ion thermal diffusivity is less than predicted by conventional neoclassical theory. One possible explanation for the observed sub-neoclassical ion thermal diffusivity is that the measured ion pressure gradient scale length is comparable to or less than the ion poloidal gyroradius, violating the assumptions of standard neoclassical theory. The strong pressure gradient is predicted to produce a large radial electric field gradient which squeezes the ion banana orbit, reducing neoclassical transport[26]. Other potential explanations include the existence of a thermal pinch or an anomalous ion-electron thermal equilibration. Recent analysis of neoclassical theory[27] with the poloidal ion gyroradius comparable to the pressure gradient scale length has found the trapped particle fraction and banana width are modified. The resulting effect is to reduce significantly the neoclassical ion thermal diffusivity, by as much as two orders of magnitude in the plasma core, which is also shown in Fig. 6.

The systematic and statistical uncertainties of the transport coefficients have been estimated. Their statistical variation over a period of 200 ms is used to determine the statistical standard deviation of the transport coefficients, which are computed every 10 ms. The systematic uncertainty is determined from the propagation of the systematic uncertainties of the input data in the transport equations. The uncertainties shown in Figs. 5 and 6 reflect the combined statistical and systematic uncertainties.

Neoclassical momentum diffusivity is predicted[28] to be much lower than neoclassical ion thermal diffusivity. However measurements from TFTR[29,30] supershot and L-mode plasmas find the momentum diffusivity profile is approximately equal to the ion thermal diffusivity and hence much larger than the predicted neoclassical momentum diffusivity. Theories based on electrostatic turbulence[31] or non-Maxwellian ion distribution[32] have been proposed to explain the observations of enhanced momentum diffusivity. Measurement of the momentum diffusivity in an ERS plasma provides independent confirmation of the reduced ion thermal diffusivity in ERS plasmas, which does not depend on thermal pinches or ion-electron energy exchange, as well as provide insight into the mechanism driving the enhanced ion and momentum diffusivity. Experiments have been done on TFTR with beam co-injection and counter to the plasma current in the low power (5-15 MW) postlude phase. With unbalanced

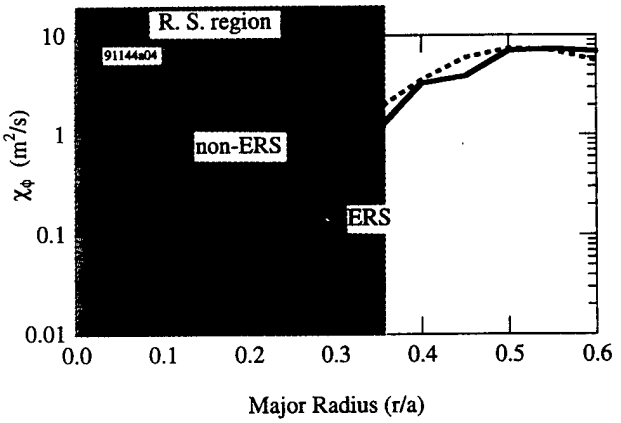

FIG. 7. Momentum diffusivity profile during the ERS-mode (solid line) and after a transition out of the ERS-mode (dashed line).

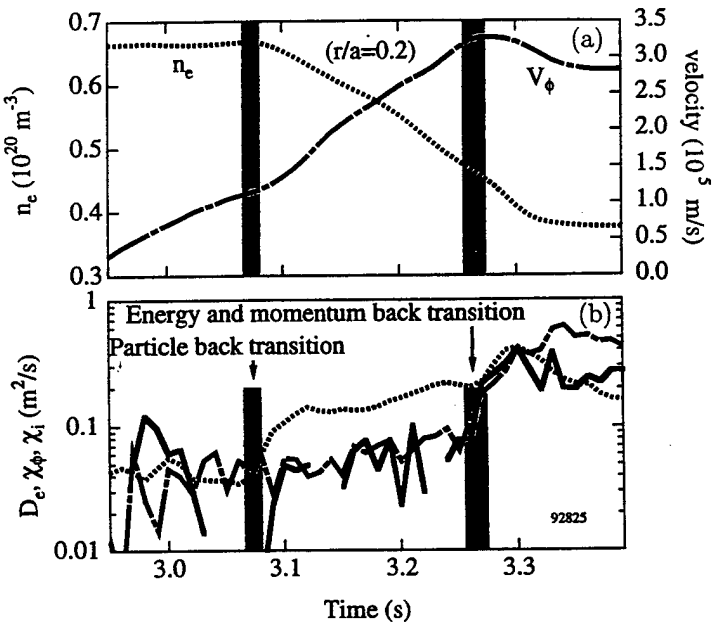

FIG. 8. (a) Time evolution of the electron density (dotted line) and rotation velocity (dashed–dotted line) at r/a = 0.2. (b) Temporal evolution of the particle (dotted line), ion thermal (solid line), and momentum diffusivity (dashed–dotted line) at r/a = 0.2 during the low power (7 MW) phase.

beam injection the toroidal velocity of the plasma increases rapidly during the ERS-mode, resulting in a calculated χ_ϕ that is reduced, consistent with the reduction in χ_i. After the transitions out of the ERS-mode, χ_ϕ increases to a much larger level. The χ_ϕ profiles during the ERS mode and after a transition out of the ERS mode are shown in Fig. 7. The time of the back transition of χ_ϕ and χ_i, out of the ERS-mode is also in good agreement. However, the particle diffusivity makes a transition out of the ERS-mode 50-200 ms before χ_ϕ and χ_i. The time evolution of the electron density and rotation velocity at $r/a = 0.2$ is shown in Fig. 8(a). The density has a clear back transition at 3.08 seconds when it begins to decrease. The corresponding electron particle diffusivity also shows a sharp increase at that time (Fig. 8(b)). The toroidal rotation velocity continues to accelerate during this time until 3.26 seconds when it abruptly stops accelerating and begins to slow down. The corresponding momentum diffusivity rises indicating the momentum diffusivity back transition is almost 0.2 seconds after the particle diffusivity back transition. The ion thermal diffusivity rises at the same time the momentum diffusivity increases, shown in Fig. 8(b). The start of reduced χ_i into the ERS-mode appears to occur at about the same time as the reduction of the particle diffusivity. However, the particle diffusivity appears to decrease more rapidly. This suggests the physical mechanism responsible for driving the particle transport is not the same as that causing the ion thermal and momentum transport.

The electron temperature increases and the profile is broader in ERS plasmas. This can be accounted for by the increased electron heating from ion-electron energy exchange due to the higher density. This results in little if any change in the inferred electron thermal diffusivity, χ_e.

6. Transition Physics

The underlying physics of the ERS transition has been a subject of study on TFTR. Analysis with a comprehensive gyrofluid simulation[33] has found that the dominant instability is the trapped electron mode (TEM). Stabilization can occur due to the reversed magnetic shear and Shafranov shift effects, which reverse the direction of the toroidal drift precession of barely trapped electrons so that the resonances that drive the TEM are eliminated. Another possible mechanism that can lead to reduced turbulence is flow shear[34], driven by gradients in the radial electric field that are generated by pressure and velocity gradients. A positive feedback mechanism involving pressure gradient driven flow shear stabilization has also recently been proposed[35]. Comparison of the $\gamma_{E\times B}$ flow shear stabilization and the maximum linear growth rate indicates qualitative agreement when $\gamma_{E\times B} > \gamma^{max}$[36,37]. The flow shear is defined as $\gamma_{E\times B} = \frac{RB_\theta}{B}\frac{d}{dR}\frac{E_r}{RB_\theta}$[38], where E_r is evaluated by solving the radial component of the force balance equation for carbon ions, $E_r = \frac{1}{n_i e Z}\nabla p_i + V_\phi B_\theta - V_\theta B_\phi$, where p_i is the carbon pressure and V_ϕ the toroidal velocity measured with

charge exchange spectroscopy, B_ϕ is the toroidal field, and B_θ is the poloidal field measured with MSE. The poloidal velocity, V_θ, is evaluated using a comprehensive numerical calculation[39].

The flow shear model has been tested on TFTR using co/counter-injected neutral beams to control the toroidal velocity profile and hence the radial electric field profile. This will affect the velocity driven contribution to the radial electric field but not the pressure driven part. By varying the amount and direction of rotation, the velocity contribution to the radial electric field can either increase the total electric field (counter-injection) or decrease the electric field (co-injection). Shown in Fig. 9(a) is the time evolution of the central density for three discharges that have different fractions of co-injected power at constant total power, 15 MW. The time of the transition out of the ERS mode occurs later as the counter-injected fraction is increased. This is consistent with $E_r \times B$ flow shear which, as shown in Fig. 9(b), decreases earlier with co-injection fraction as a result of the reduced electric field shear. Direct comparison of the shearing rates to the maximum linear growth rate indicates that the back transitions occur when $\gamma_{E_r \times B} \sim (0.5 - 1)\gamma^{max}$, consistent with the shear suppression criterion of Ref.[36]. However, the start of the ERS-mode is not consistent with this model. The transition threshold favors near balanced injection. In conditions

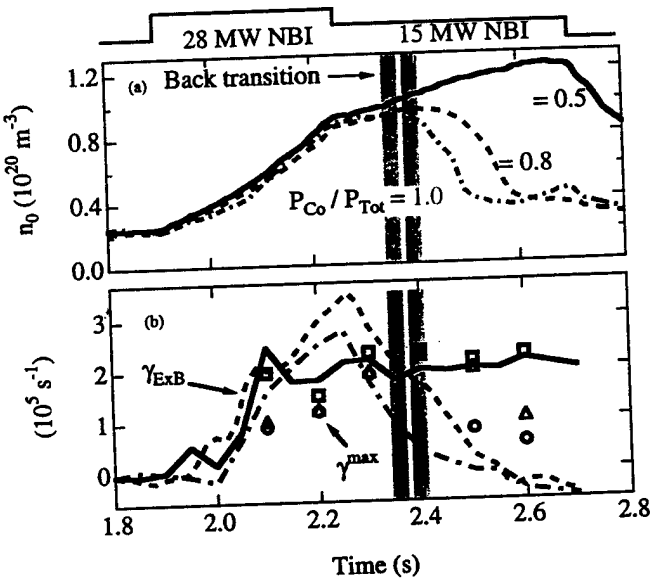

FIG. 9. (a) Time evolution of the central density with co-injected fractions of 1.0 (dashed-dotted line), 0.8 (dashed line) and 0.5 (solid line). (b) Corresponding evolution of flow shear and growth rate for co-injected fractions of 1.0 (circles), 0.8 (triangles) and 0.5 (squares).

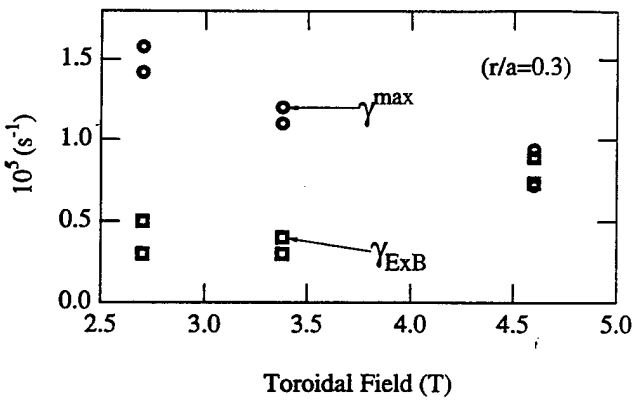

FIG. 10. Linear growth rates (circles) and flow shear rates (squares) for various toroidal magneti fields at the time of the ERS-mode transition.

where the flow shear exceeds the growth rate, transitions do not occur if the beams are strongly co- or counter dominated. Conversely, in a toroidal magnetic field scan, which shows that the threshold is a strong function of B_ϕ, the power threshold is found to be lower than predicted by the flow shear model at magnetic fields lower than 4.6 T. Shown in Fig. 10 are the shearing and growth rates just before an ERS transition as the toroidal magnetic field is varied. At high toroidal magnetic field the two terms are about equal just before the transition occurs, but at lower toroidal magnetic field the shearing rate is much less than the growth rate.

7. Conclusion

In conclusion, highly peaked density and pressure profiles in a new reversed shear operating regime have been observed on TFTR. The particle transport is reduced to roughly the neoclassical level, and the ion thermal diffusivity is well below predictions from conventional neoclassical theory. As in supershots, the momentum diffusivity is observed to remain approximately equal to the ion thermal diffusivity. Little or no change is seen in the electron thermal diffusivity. A possible explanation for the inferred sub-neoclassical ion thermal diffusivity is the violation of the assumptions of standard neoclassical theory. A modified neoclassical analysis reduces the standard neoclassical ion thermal diffusivity significantly. The improved transport is observed throughout the region of reversed shear and is found to broaden as r_{min} is increased. The mechanism of transport suppression is a question of fundamental importance in understanding tokamak transport and developing the tokamak, or some other magnetic confinement concept, into an attractive reactor. Experimental and theoretical studies to date point to stabilization of the trapped electron mode by a combination of reversed shear, Shafranov shift, and radial electric field shear.

The model agrees well with the back transition data, but the simple shear flow model is not consistent with the power threshold results dependence on toroidal magnetic field. Further improvements of the models including nonlinear simulations incorporating $E_r \times B$ are needed, but comparison of data to models would greatly benefit with a direct measurement of the E_r profile. Neoclassical transport is usually thought to be the minimum transport possible, and these results represent a dramatic improvement in confinement and performance. With the low transport coefficients found in the ERS-mode, dramatic improvements in the performance of present and future tokamak reactors may be possible if the improved confinement can be achieved in an MHD stable regime with a large bootstrap current consistent with the desired current profile.

We would like to thank the TFTR staff for their support and operation of TFTR and W. Houlberg for the use of his code for calculating the neoclassical transport. This work was supported by United States Department of Energy Contract No. DE-AC02-76-CHO-3073.

REFERENCES

[1] KESSEL, C., MANICKAM, J., REWOLDT, G., TANG, W.M., Phys. Rev. Lett. **72** (1994) 1212.
[2] KADOMTSEV, B.B., POGUTSE, O.P., Sov. Phys. JETP **24** (1967) 1172.
[3] ROSENBLUTH, M., SLOAN, M.L., Phys. Fluids **14** (1971) 1725.
[4] SYKES, A., WESSON, J.A., COX, S.J., Phys. Rev. Lett. **39** (1977) 757.
[5] GOLDSTON, R.J., et al., Plasma Phys. Control. Fusion **36** (1994) B213.
[6] JET TEAM, in Plasma Physics and Controlled Nuclear Fusion Research 1988 (Proc. 12th Int. Conf. Nice, 1988), Vol. 1, IAEA, Vienna (1989) 215.
[7] MOREAU, D., et al., in Plasma Physics and Controlled Nuclear Fusion Research 1992 (Proc. 14th Int. Conf. Würzburg, 1992), Vol. 1, IAEA, Vienna (1993) 649.
[8] STRAIT, E.J., et al., Phys. Rev. Lett. **75** (1995) 4421.
[9] LAZARUS, E.A., et al., Phys. Fluids B **3** (1991) 2221.
[10] ISHIDA, S., et al., Phys. Rev. Lett. **68** (1992) 1531.
[11] KESNER, J., et al., Phys. Fluids B **5** (1993) 2525.
[12] POLITZER, P.A., et al., Phys. Plasmas **1** (1994) 1545.
[13] MEADE, D.M., et al., in Plasma Physics and Controlled Nuclear Fusion Research 1990 (Proc. 13th Int. Conf. Washington, DC, 1990), Vol. 1, IAEA, Vienna (1991) 9.
[14] LEVINTON, F.M., et al., Phys. Rev. Lett. **75** (1995) 4417.
[15] LEVINTON, F.M., et al., Phys. Rev. Lett. **63** (1989) 2060.
[16] LEVINTON, F.M., Rev. Sci. Instrum. **63** (1992) 5157.
[17] HIRSHMAN, S.P., et al., Phys. Plasmas **1** (1994) 2277.
[18] HAWRYLUK, R.J., in Proc. Course on Physics of Plasmas Close to Thermonuclear Conditions, Varenna, 1979, Vol. 1, European Commission, Brussels (1980) 19.
[19] BATHA, S.H., LEVINTON, F.M., HIRSHMAN, S.P., BELL, M.G., WIELAND, R.M., Nucl. Fusion **36** (1996) 1133.
[20] ZARNSTORFF, M.C., LEVINTON, F.M., BATHA, S.H., SYNAKOWSKI, E.J., The effect of E_r on MSE measurements of q, a new technique for measuring E_r, and a test of the neoclassical electric field, Phys. Plasmas (in press).

[21] STRACHAN, J.D., et al., Phys. Rev. Lett. 58 (1987) 1004.
[22] MAZZUCATO, E., et al., Phys. Rev. Lett. 77 (1996) 3145.
[23] EFTHIMION, P.C., et al., Phys. Rev. Lett. 75 (1995) 85.
[24] ZARNSTORFF, M.C., et al., in Plasma Physics and Controlled Nuclear Fusion Research 1988 (Proc. 12th Int. Conf. Nice, 1988), Vol. 1, IAEA, Vienna (1989) 183.
[25] CHANG, C.S., HINTON, F.L., Phys. Fluids 29 (1986) 3314.
[26] SHAING, K.C., HSU, C.T., HAZELTINE, R.D., Phys. Plasmas 1 (1994) 3365.
[27] LIN, Z., TANG, W.M., LEE, W.W., Phys. Rev. Lett. 78 (1997) 456.
[28] ROSENBLUTH, M.N., RUTHERFORD, P.H., TAYLOR, J.B., FRIEMAN, E.A., KOVRIZHNYKH, L.M., in Plasma Physics and Controlled Nuclear Fusion Research 1971 (Proc. 4th Int. Conf. Madison, 1971), Vol. 1, IAEA, Vienna (1971) 495.
[29] SCOTT, S.D., et al., in Plasma Physics and Controlled Nuclear Fusion Research 1988 (Proc. 12th Int. Conf. Nice, 1988), Vol. 1, IAEA, Vienna (1989) 655.
[30] SCOTT, S.D., et al., Phys. Rev. Lett. 64 (1990) 531.
[31] MATTOR, N., DIAMOND, P.H., Phys. Fluids 31 (1988) 1180.
[32] WARE, A.A., Phys. Rev. Lett. 64 (1990) 2655.
[33] BEER, M.A., PhD Thesis, Princeton Univ., NJ (1995).
[34] BIGLARI, H., DIAMOND, P.H., TERRY, P.W., Phys. Fluids B 2 (1990) 1.
[35] DIAMOND, P.H., et al., On the transition to enhanced confinement in reversed magnetic shear discharges (in preparation).
[36] WALTZ, R.E., KERBEL, G.D., MILOVICH, J., Phys. Plasmas 1 (1994) 2229.
[37] WALTZ, R.E., KERBEL, G.D., MILOVICH, J., HAMMETT, G.W., Phys. Plasmas 2 (1995) 2408.
[38] HAHM, T.S., BURRELL, K.H., Phys. Plasmas 2 (1995) 1648.
[39] HOULBERG, W., SHAING, K.C., HIRSHMAN, S.P., ZARNSTORFF, M.C., Bootstrap current and neoclassical transport in tokamaks of arbitrary collisionality and aspect ratio (in preparation).

DISCUSSION

K. LACKNER: Do any of the theoretical ideas you mentioned offer an explanation for the observation of distinct back-transitions for particle and energy/momentum diffusivities?

F.M. LEVINTON: No, but we have recently begun looking into possible explanations.

V. PARAIL: The fact that you see different transitions for density and ion momentum flow probably indicates that particle transport is controlled by the electrons. In this case you should see a sudden change in the radial electric field. Did you find this kind of electric field modification?

F.M. LEVINTON: We have not yet looked into this possibility.

K. IDA: If the $\mathbf{E} \times \mathbf{B}$ velocity shear driven by the pressure gradient plays an important role in an ERS discharge, the improvement of transport (reduction of χ_i) should be slow. Do you see a gradual change of χ_i after the transition from L mode to ERS mode? The back-transition from ERS to L mode depends on beam configuration (co- or balanced injection). The transition from L mode to ERS should be affected by the beam configuration, and a faster increase in $\gamma_{E\times B}$ should be predicted for balanced

than for co-injection. Are there differences in delay time for the transition ıode to ERS after the high power NBI is turned on, between co- and balanced ?

1. LEVINTON: Yes, we see a gradual decrease in the ion thermal transport. the transition occurs with balanced beams at lower power. However, the time ansitions is about the same for both cases.

Report Number (14) ORNL/CP--94704
CONF-971010--
IAEA-CN--64/A1-3

Publ. Date (11) 199709
Sponsor Code (18) DOE/ER, XF
UC Category (19) UC-400, DOE/ER

DOE